Pramana – J. Phys. (2019) 92:17
https://doi.org/10.1007/s12043-018-1690-2

Heat transfer enhancement for Maxwell nanofluid flow subject to convective heat transport

M KHAN[1], M IRFAN[1,*] and W A KHAN[2]

[1]Department of Mathematics, Quaid-i-Azam University, Islamabad 44000, Pakistan
[2]Department of Mathematics, Hazara University, Mansehra 21300, Pakistan
*Corresponding author. E-mail: mirfan@math.qau.edu.pk

MS received 15 March 2018; revised 9 June 2018; accepted 12 June 2018; published online 2 January 2019

Abstract. Nanoliquids possess remarkable features that have fascinated numerous researchers because of their utilisation in nanoscience and nanotechnology. A mathematical relation for the two-dimensional flow of Maxwell nanoliquid over a stretching cylinder is established. Buongiorno's relation is considered here to visualise the impact of Brownian moment and thermophoresis mechanisms on Maxwell liquid. The convective heat transport is deliberated for heat transfer mechanisms. Transformation procedure yields nonlinear differential system which is then computed through the homotopic approach. The results obtained are studied in detail in relation to somatic parameters. It is notable that the velocity of Maxwell liquid shows conflicting behaviour for curvature parameter α and Deborah number β. Moreover, the liquid temperature increases for increased values of Brownian motion N_b and thermophoresis parameter N_t. Additionally, the authentication of numerical consequences is prepared via benchmarking with formerly identified restrictive circumstances and we initiate a splendid communication with these results.

Keywords. Maxwell fluid; nanofluid; stretching cylinder; Brownian and thermophoresis nanoparticles; convective condition.

PACS Nos **44.10.+i; 47.61.−K; 87.85.Rs**

1. Introduction

The transport of heat is the most significant mechanism in several consumer and industrial products. Researchers have made great efforts to improve the poor thermal conductivity of conventional liquids. With rapid improvement of technology and science worldwide, improving the efficiency of transfer of energy and energy saving are posing new challenges. Utilising innovative materials is among the most extensively adopted techniques for heat transfer efficiency. Moreover, traditional heat transfer liquids could not meet special requirements such as strong intensity of heat transfer. On exploring and scrutinising nanoparticles, Choi [1] has coined the term 'nanofluids'. Nanofluid, as an innovative generation of superoperative medium, has been rapidly emerging as a new medium to increase the heat transfer coefficient of conventional liquids. The improvement of nanoliquids has occurred as an impulsive trend, particularly in the past. The field of analysis of nanoliquids has intricate constancy analysis, somatic assets amounts, steaming heat transfer, mass transfer, industrial solicitation and few notional analysis or model growths. Nanoliquids comprise solid nanofibres or nanoparticles with a size of 1–100 nm. Nanoliquids have advanced thermal conductivity compared to conventional heat transfer liquids that allows for their broad application in areas of heat exchange and astrophysical energy structure. Until now, several broad theories have been proposed on the thermophysical assets and heat transfer of nanoliquids of altered base fluids [2–13]. For instance, the influence of chemical species on two-dimensional (2D) radiative flow of Burgers nanoliquid was explored by Khan *et al* [14]. Convective heat structure and nanoparticle mass flux conditions were also deliberated over. Hayat *et al* [15] inspected the influence of Newtonian heating in nanoliquids over a permeable cylinder. They established that the stimulus of suction/injection and curvature parameters on coefficient of skin friction is analogous. Flow scrutiny of nanoliquids using a porous stretched cylinder was deliberated by Nourazar *et al*

[16]. The impact of nonlinear radiative and magneto Eyring–Powell nanoliquid flow by utilising the innovative mass flux condition was examined numerically by Khan *et al* [17]. They noted that the nanoliquid temperature has been enhanced for thermal radiation and Biot number. An assessment of two numerical techniques, namely bvp4c and shooting scheme was also presented in this study. Recently, Ellahi [18] discussed the special and advanced progress on nanofluids. The impact of chemical reaction and activation energy in Couette–Poiseuille nanofluid flow with convective condition was analysed by Zeeshan *et al* [19]. They showed that the effect of thermophoresis parameter and Brownian motion on concentration field displays opposite trend. The analysis of time-dependent Williamson nanofluid in the manifestation of chemical reaction with activation energy was reported by Hamid *et al* [20].

Numerous experimental, analytical and numerical mechanisms have been envisioned to explore the impact of nonlinear materials over a stretching cylinder. The flow analysis of stretching cylinder has various practical applications in engineering and trade such as cord illustration, spinning of metallic, piping, methods of extrusion in metallurgy, sophistication of rough oil, production of elastic, glaze of cylinder-shaped cords and crust and so forth. Crane [21] has inspected the flow by a stretched cylinder. Afterwards Wang [22] conferred the steady viscous liquid flow in an ambient liquid at rest exterior to a stretched hollow cylinder. Later on, Wang and Ng [23] described the slip flow influenced by a stretching cylinder. This exploration showed that slip critically diminishes velocities and shear stress. Flow and heat transfer analysis with stagnation point due to shrinking/stretching cylinder was considered by Markin *et al* [24]. This study exposed that for large curvature parameter augments the heat transfer amount at surface. The radiative flow of a magneto Eyring–Powell nanoliquid induced by a stretched cylinder was studied by Hayat *et al* [25]. Numerically, the impact of thermally stratified and magnetohydrodynamics (MHD) on Casson liquid over a stretched cylinder was analysed by Rehman *et al* [26]. They reported that the local Nusselt number is a declining function of the Casson liquid parameter while the reverse trend is noticed for curvature parameter.

In numerous applications, the flow features of non-Newtonian liquids have unexpected impact, including polymers, fraternisation, exposure, dispensing, trial assortment and split-up of innumerable biological and chemical sorts on a microchip. The remarkable characteristics of these fluids are their higher apparent viscosities such that the laminar flow shows a habitual increase when associated with Newtonian fluids and the Prandtl numbers, which is surprising. The nature of these fluids is multifaceted and cannot be determined by single constitute equation. The constitutive associations of such liquids are pointedly wide ranging and intricate compared to the viscous liquids. Numerous non-Newtonian liquid models have been studied previously [27–29]. Hayat *et al* [30] reported the importance of carbon nanotubes in Darcy–Forchheimer flow. They found that for curvature parameter the velocity and temperature fields are enriched. Recently, Khan *et al* [31] described the properties of advanced heat conduction theory with homogeneous and heterogeneous reactions in a three-dimensional Carreau fluid. They observed that for both shear thickening and thinning liquids, the performance of local Weissenberg numbers is quite conflicting on the concentration field.

From the aforementioned studies, it can be seen that there have been no attempts to explore the flow of a Maxwell nanoliquid by a stretching cylinder. A new modelling for 2D Maxwell fluid flow is established over a stretching cylinder by utilising the boundary layer estimate. The governing partial differential equations (PDEs) are altered into ordinary differential equations (ODEs) via apposite conversion and then tackled analytically by means of the homotopic approach (homotopy analysis method (HAM)) [32–35]. Some tables are given and graphs are plotted for various parameters.

2. Mathematical formulation

Consider a steady 2D flow of the Maxwell nanoliquid influenced by a stretched cylinder of radius R. The Brownian and thermophoresis parameters are described for heat and mass transfer mechanisms. Moreover, the convective heat transport is also considered. The cylinder is stretched with velocity $U_0 z/l$ along the z-direction, where U_0 is the reference velocity and l is the specific length. Let cylindrical polar coordinates (z, r) are taken in such a way that the z-axis goes beside the axis of the cylinder and the r-axis is restrained along the radial direction, as shown in figure 1. Furthermore,

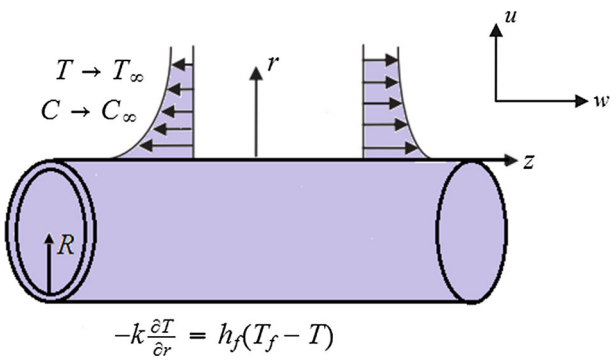

Figure 1. Schematic diagram.

it is presumed that at the surface of the cylinder, T_f, C_f, respectively, are the liquid temperature and nanoparticle fraction, and T_∞, C_∞ are the ambient temperature and nanoparticle fraction, respectively. The equations under the estimated boundary layer for the Maxwell nanofluid model [36,37], in natural representation, are given as follows:

$$\frac{\partial u}{\partial r}+\frac{u}{r}+\frac{\partial w}{\partial z}=0, \tag{1}$$

$$u\frac{\partial w}{\partial r}+w\frac{\partial w}{\partial z}+\lambda\left[w^2\frac{\partial^2 w}{\partial z^2}+u^2\frac{\partial^2 w}{\partial r^2}+2uw\frac{\partial^2 w}{\partial r\partial z}\right]=\nu\left[\frac{\partial^2 w}{\partial r^2}+\frac{1}{r}\frac{\partial w}{\partial r}\right], \tag{2}$$

$$u\frac{\partial T}{\partial r}+w\frac{\partial T}{\partial z}=\alpha_1\left[\frac{\partial^2 T}{\partial r^2}+\frac{1}{r}\frac{\partial T}{\partial r}\right]+\tau\left[D_B\frac{\partial C}{\partial r}\frac{\partial T}{\partial r}+\frac{D_T}{T_\infty}\left(\frac{\partial T}{\partial r}\right)^2\right], \tag{3}$$

$$u\frac{\partial C}{\partial r}+w\frac{\partial C}{\partial z}=D_B\frac{1}{r}\frac{\partial}{\partial r}\left[\left(r\frac{\partial C}{\partial r}\right)\right]+\frac{D_T}{T_\infty}\frac{1}{r}\frac{\partial}{\partial r}\left[\left(r\frac{\partial T}{\partial r}\right)\right], \tag{4}$$

with boundary conditions

$$w(r,z)=W(z)=\frac{U_0 z}{l},\quad u(r,z)=0,$$

$$-k\frac{\partial T}{\partial r}=h_f\left(T_f-T\right),\quad C=C_f\quad \text{at}\quad r=R, \tag{5}$$

$$w\to 0,\quad T\to T_\infty,\quad C\to C_\infty\quad \text{as}\quad r\to\infty. \tag{6}$$

Here u, w are the velocity components in the r- and z-directions, respectively, ν is the kinematics viscosity, λ is the relaxation time, T, C are the liquid temperature and concentration, respectively, $\alpha_1=(k/(\rho c)_f)$ are the nanoliquid thermal diffusivity, in which ρ_f, c_f are the density of liquid and specific heat, respectively, and k is the thermal conductivity of the liquid, τ is the ratio of effective heat capacity of the nanoparticle material to the heat capacity of the base liquid, D_B, D_T are the Brownian diffusion and thermophoresis diffusion coefficients, respectively, and h_f is the heat conversion coefficient.

Presenting the following conversions

$$u=-\frac{R}{r}\sqrt{\frac{U_0\nu}{l}}f(\eta),\quad w=\frac{U_0 z}{l}f'(\eta),$$

$$\theta(\eta)=\frac{T-T_\infty}{T_f-T_\infty},$$

$$\phi(\eta)=\frac{C-C_\infty}{C_f-C_\infty},\quad \eta=\sqrt{\frac{U_0}{\nu l}}\left(\frac{r^2-R^2}{2R}\right) \tag{7}$$

and after substituting the overhead conversions, eq. (1) is satisfied automatically and eqs (2)–(6) yield

$$(1+2\alpha\eta)f'''+2\alpha f''+ff''-f'^2+2\beta ff'f''-\beta f^2 f'''-\frac{\alpha\beta}{(1+2\alpha\eta)}f^2 f''=0, \tag{8}$$

$$(1+2\alpha\eta)\theta''+2\alpha\theta'+\mathrm{Pr}\,f\theta'+(1+2\alpha\eta)\,\mathrm{Pr}\,N_\mathrm{b}\theta'\phi'+(1+2\alpha\eta)\,\mathrm{Pr}\,N_\mathrm{t}\theta'^2=0, \tag{9}$$

$$(1+2\alpha\eta)\phi''+2\alpha\phi'+\mathrm{Le}\,\mathrm{Pr}\,f\phi'+(1+2\alpha\eta)\left(\frac{N_\mathrm{t}}{N_\mathrm{b}}\right)\theta''+2\alpha\left(\frac{N_\mathrm{t}}{N_\mathrm{b}}\right)\theta'=0, \tag{10}$$

$$f(0)=0,\quad f'(0)=1,\quad \theta'(0)=-\gamma(1-\theta(0)),$$

$$\phi(0)=1, \tag{11}$$

$$f'(\infty)=0,\quad \theta(\infty)=0,\quad \phi(\infty)=0, \tag{12}$$

where $\alpha\,(=(1/R)\sqrt{\nu l/U_0})$ is the curvature parameter, $\beta\,(=(\lambda U_0/l))$ is the Deborah number, Pr $(=\nu/\alpha_1)$ is the Prandtl number, $N_\mathrm{b}\,(=(\tau D_B(C_f-C_\infty))/\nu))$ is the Brownian motion parameter, $N_\mathrm{t}\,(=(\tau D_T(T_f-T_\infty))/\nu T_\infty)$ is the thermophoresis parameter, Le $(=(\alpha_1/D_B))$ is the Lewis number and $\gamma\,(=(h_f/k)\sqrt{\nu l/U_0})$ is the Biot number.

3. Engineering and industrial quantities of interest

The expressions for the local Nusselt number (Nu_z) and local Sherwood number (Sh_z) are

$$\mathrm{Nu}_z=\frac{zq_m}{k(T_f-T_\infty)},\quad \mathrm{Sh}_z=\frac{zj_m}{D_B(C_f-C_\infty)}, \tag{13}$$

where q_m and j_m are the heat and mean flux, respectively,

$$q_m=-k\left(\frac{\partial T}{\partial r}\right)_{r=R},\quad j_w=-D_B\left(\frac{\partial C}{\partial r}\right)_{r=R}. \tag{14}$$

The dimensionless form of eq. (13) is given by

$$\mathrm{Nu}_z\mathrm{Re}_z^{-1/2}=-\theta'(0),\quad \mathrm{Sh}_z\mathrm{Re}_z^{-1/2}=-\phi'(0), \tag{15}$$

where $\mathrm{Re}_z=W(z)z/\nu$ is the local Reynolds number.

4. Homotopic results

In this section, we are trying to achieve the series solutions of the considered problem through the homotopic approach and we decide on initial estimates and linear operators for flow problems. Therefore, the initial guesses (f_0,θ_0,ϕ_0) with auxiliary linear operators $(\pounds_f,\pounds_\theta,\pounds_\phi)$ can be written as

$$f_0(\eta) = 1 - \mathrm{e}^{-\eta}, \quad \theta_0(\eta) = \frac{\gamma}{1+\gamma}\mathrm{e}^{-\eta},$$
$$\phi_0(\eta) = \mathrm{e}^{-\eta}, \tag{16}$$
$$\pounds_f[f(\eta)] = f''' - f', \quad \pounds_\theta[\theta(\eta)] = \theta'' - \theta,$$
$$\pounds_\phi[\phi(\eta)] = \phi'' - \phi. \tag{17}$$

5. Convergence analysis

We identified that in HAM the supporting $\hbar_f$, $\hbar_\theta$ and $\hbar_\phi$ are precisely authoritative to adjust and alter the convergence of the series solutions. The appropriate value of these supporting parameters is proposed by seeing the least-squares error which is certain by

$$F_{f,m} = \frac{1}{N+1}\sum_{j=0}^{N}\left[N_f \sum_{i=0}^{m} F_j(i\Delta\eta)\right]^2. \tag{18}$$

Table 1 shows the convergence of the series solution and it can be seen that the convergent solution for the velocity is attained at the 14th order of the estimate, whereas such a convergence for nanoliquid temperature and concentration is attained at the 18th order of estimate.

Table 1. Convergence of homotopy solutions when $\alpha = \beta = 0.1$, $\mathrm{Pr} = 2.0$, $N_\mathrm{b} = 0.3$, $N_\mathrm{t} = \gamma = 0.2$ and $\mathrm{Le} = 1.0$ are fixed.

Order of estimate	$-f''(0)$	$-\theta'(0)$	$-\phi'(0)$
1	1.05454	0.159789	0.883330
4	1.06206	0.154158	0.876878
8	1.06170	0.153596	0.881523
12	1.06168	0.153577	0.881703
16	1.06162	0.153576	0.881727
20	1.06162	0.153575	0.881728
25	1.06162	0.153575	0.881728

6. Analysis of results

The main focus of this section is to confer the stimulus of the inserting parameters on the velocity component, the temperature and concentration fields through the homotopic approach. The results for seeming somatic parameters are schemed and conferred.

6.1 *Impact of curvature parameter α on $f'(\eta)$, $\theta(\eta)$ and $\phi(\eta)$*

Figures 2a–2c show the influence of curvature parameter α on velocity component, nanoliquid temperature and concentration of Maxwell liquid. It is reported that the velocity of Maxwell liquid, nanoliquid temperature and concentration fields increase for increasing values of α. Physically, the radius of curvature decreases, decreasing the interaction region of the cylinder with the liquid. Consequently, the resistance offered by the exterior declines and the velocity of Maxwell liquid increases. Furthermore, it is noted that higher values of α increase both the temperature and its allied thermal thickness of the boundary layer. Hence, the heat transport decreases and the temperature of Maxwell nanoliquid increases.

6.2 *Impact of Deborah number β on $f'(\eta)$, $\theta(\eta)$ and $\phi(\eta)$*

The stimulus of Deborah number β on velocity component, temperature and concentration distribution is portrayed in figures 3a–3c. From these interpretations, intensification in β declines both the velocity and temperature of Maxwell liquid while reverse trend is being

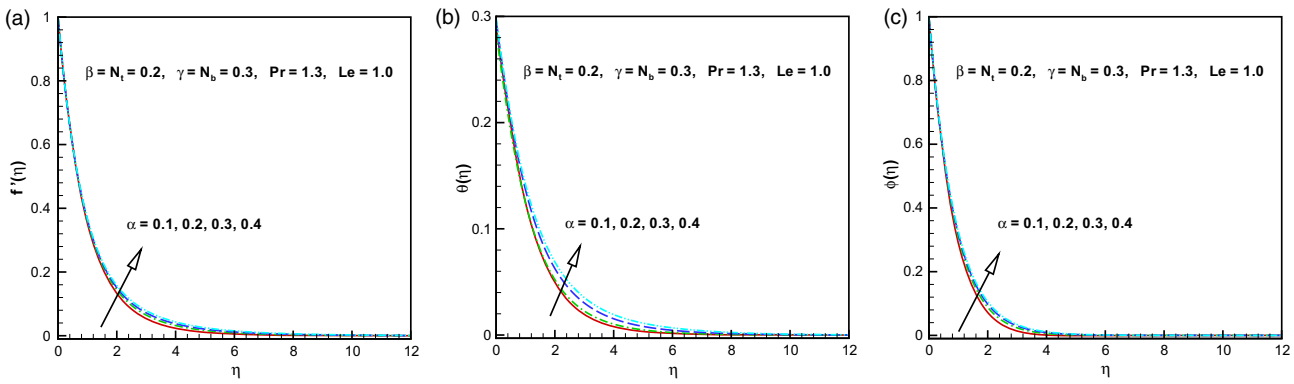

Figure 2. Influence of the curvature parameter α on (**a**) velocity, (**b**) temperature and (**c**) concentration fields.

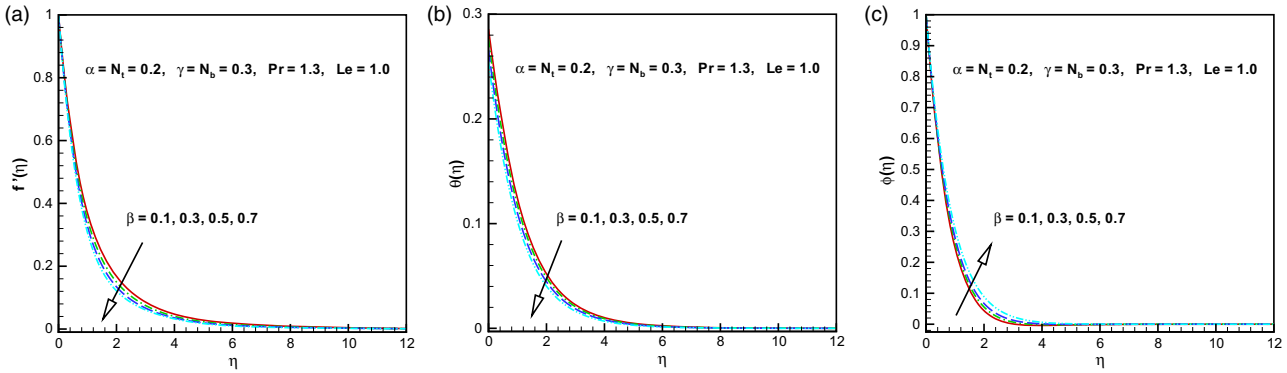

Figure 3. Influence of the Deborah number β on (**a**) velocity, (**b**) temperature and (**c**) concentration fields.

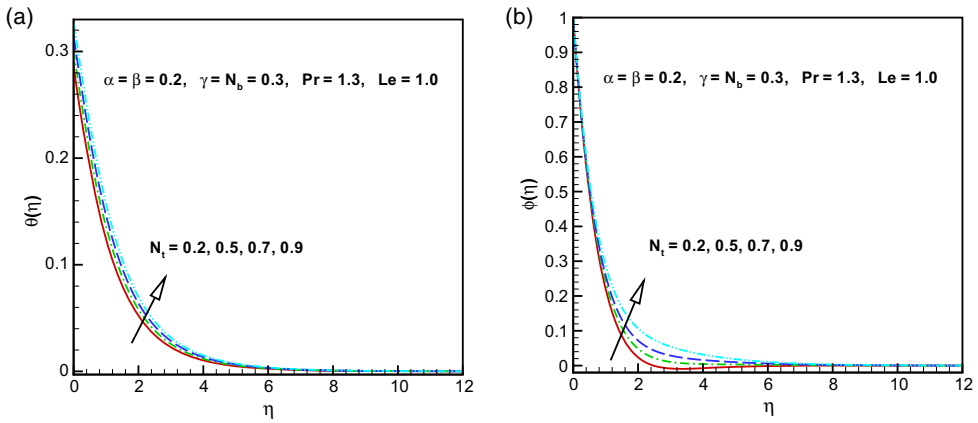

Figure 4. Influence of the thermophoresis parameter N_{t} on (**a**) temperature and (**b**) concentration fields.

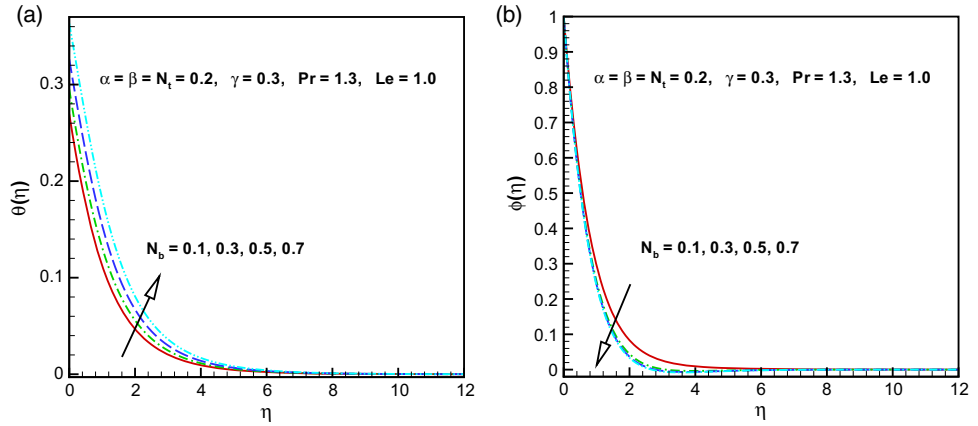

Figure 5. Influence of the Brownian motion parameter N_{b} on (**a**) temperature and (**b**) concentration fields.

identified for the concentration field. As β depends on the relaxation time, the rise in β increases the relaxation time which intensifies the liquid temperature and thermal thickness of the boundary layer as shown in figure 3a. Instead of this, the concentration of Maxwell nanoliquid increases for increasing values of β.

6.3 *Impact of thermophoresis N_{t} and Brownian motion N_{b} on $\theta(\eta)$ and $\phi(\eta)$*

Figures 4a, 4b and 5a, 5b show the impact of thermophoresis N_{t} and Brownian motion parameters N_{b} on nanoliquid temperature and concentration

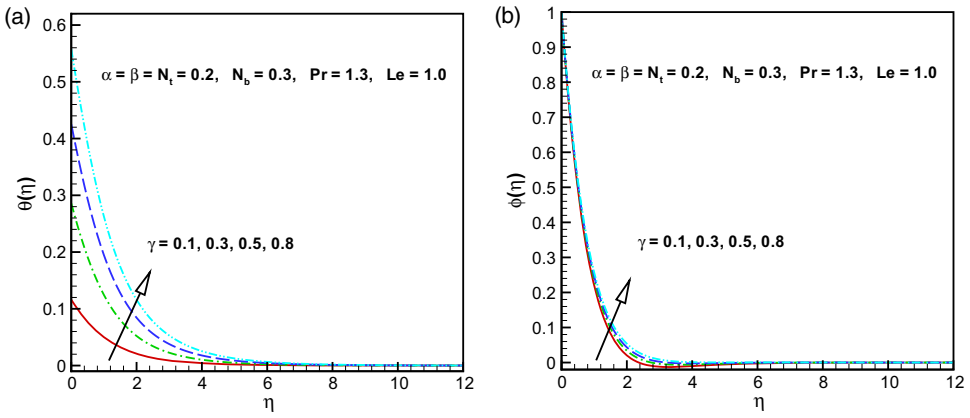

Figure 6. Influence of the Biot number γ on (**a**) temperature and (**b**) concentration fields.

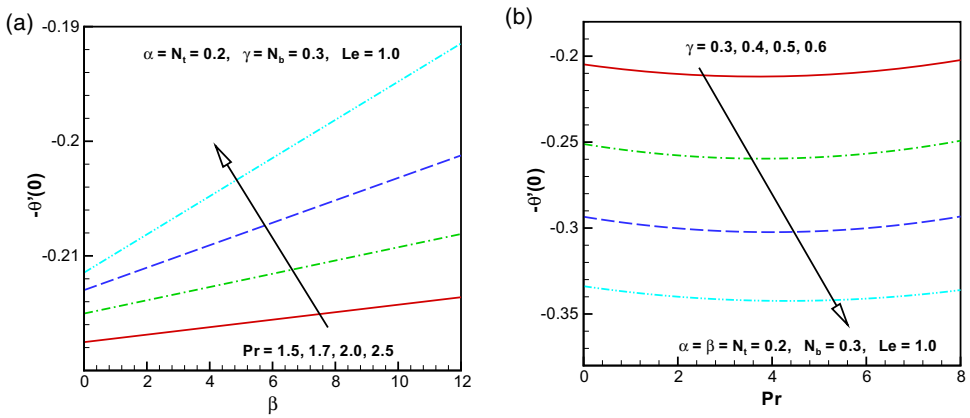

Figure 7. Influence of the Prandtl number Pr (**a**) and Biot number γ (**b**) on Nusselt number.

distribution. Similar behaviour on both the distributions are identified for intensifying the values of N_t, whereas differing tendency is being remarked for N_b on temperature and concentration fields. Physically, higher values of N_t increase the liquid temperature because the dissimilarity between wall temperature and reference temperature increases. Moreover, because of the increased value of N_t, more nanoparticles are forced away from the hot exterior. Hence, the concentration of the nanoliquid increases. On the other hand, N_b is the unsystematic association of molecules that increases and causes an enhancement of the temperature field although the concentration of Maxwell nanoliquid indicates different performance when we increase the values N_b.

6.4 *Impact of Biot number γ on $\theta(\eta)$ and $\phi(\eta)$*

To show the impact of Biot number γ on nanoliquid temperature and concentration of Maxwell fluid, figures 6a and 6b are delineated. Analogous trend is being noticed for increasing values of γ on temperature and concentration fields. The rise in the values of γ augments both the temperature and concentration of Maxwell liquid as the heat transport coefficient rises for larger γ. Thus, more heat is transferred from the heated surface of the cylinder to the cooled surface of the liquid and the liquid temperature increases which transfer additional heat from the cylinder to the liquid. Consequently, the liquid temperature increases and the reverse trend is being detected on the concentration of Maxwell nanoliquid.

6.5 *Local Nusselt number and local Sherwood number*

Figures 7a, 7b and 8a, 8b show the discrepancy of $-\theta'(0)$ in response to variation in Pr, γ, α and N_t, while figures 9a and 9b show the behaviour of $-\phi'(0)$ for altering values of Pr and γ, respectively. It can be comprehended from these plots that the heat transfer amount at the surface of the stretching cylinder decreases for Pr and γ, α and N_t, while a reverse trend is noted for increased values of Pr and γ on $-\phi'(0)$.

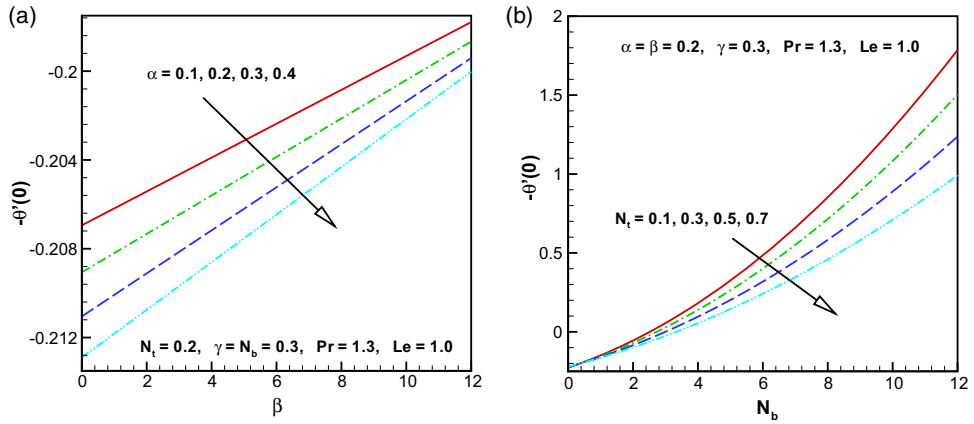

Figure 8. Influence of the curvature parameter α (**a**) and thermophoresis parameter N_t (**b**) on Nusselt number.

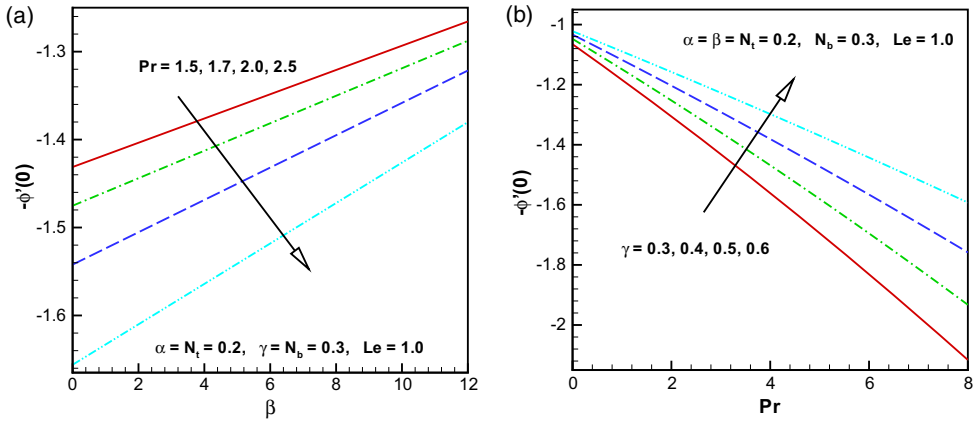

Figure 9. Influence of the Prandtl number Pr (**a**) and Biot number γ (**b**) on Sherwood number.

Table 2. Numerical computation of $-\theta'(0)$ and $-\phi'(0)$ when $\alpha = \beta = 0.1$ and $\gamma = 0.2$ are fixed.

N_t	N_b	Pr	Le	$-\theta'(0)$	$-\phi'(0)$
0.2	0.3	2.0	1.0	0.153575	0.881728
0.3				0.153015	0.856315
0.4				0.152442	0.831502
0.5				0.151849	0.807350
0.2	0.1			0.160915	0.748960
	0.2			0.157420	0.848303
	0.4			0.149360	0.898696
	0.3	1.5		0.150312	0.725672
		1.8		0.152540	0.821768
		2.5		0.155105	1.020320
		2.0	0.9	0.154065	0.820906
			1.1	0.153134	0.939455
			1.3	0.152374	1.047350

6.6 *Table of* $-\theta'(0)$ *and* $-\phi'(0)$

Table 2 presents the numerical values of $-\theta'(0)$ and $-\phi'(0)$ for fixed values of N_t, N_b, Pr and Le. The magnitude of $-\theta'(0)$ and $-\phi'(0)$ increases for higher values of Pr while it declines for N_t. Further opposite trend is being noted for higher values of N_b and Le on $-\theta'(0)$ and $-\phi'(0)$.

6.7 *Tabular comparisons*

Tables 3 and 4 are assessment tables of $-\theta'(0)$ for different values of Pr compared with some previous studies. Consequently, from these tables, we are assured that the results of this study are very precise.

Table 3. Comparison values of $-\theta'(0)$ when $\mathrm{Pr} = 1$, $\alpha = \beta = 0$, $\gamma \to \infty$, $N_b \to 0$ and $N_t = 0$.

Pr	Irfan *et al* [37]	Ishak and Nazar [38]	Elbashbeshy *et al* [39]	Poply *et al* [40]	Present
1.0	0.581977	0.5820	0.5820	0.5819	0.5819766

Table 4. Comparison values of $-\theta'(0)$ when $\alpha = \beta = 0$, $\gamma \to \infty$, $N_b \to 0$ and $N_t = 0$.

	$-\theta'(0)$				
Pr	Irfan *et al* [37]	Khan and Pop [41]	Wang [42]	Gorla and Sidawi [43]	Present
0.7	0.453933	0.4539	0.4539	0.4539	0.4539251
2.0	0.911285	0.9113	0.9114	0.9114	0.9112845

7. Concluding remarks

A mathematical analysis of the 2D flow of Maxwell nanoliquid in the manifestation of convective heat transport phenomenon influenced by a stretched cylinder has been carried out. An analytical technique, namely HAM, has been used for the elucidation of ODEs. Crucial opinions of our exploration are given below:

- The influence of curvature parameter α on velocity component, nanoliquid temperature and concentration is the same.
- Increase in the values of Deborah number β decreases the temperature of nanoliquid Maxwell field while it enhances for concentration distribution.
- The temperature of Maxwell fluid is enhanced for Brownian motion N_b and thermophoresis parameter N_t, whereas opposite behaviour is being noticed for concentration field.
- The nanoliquid temperature and the thickness of thermal boundary layer are diminishing functions of Prandtl number Pr.
- The heat transfer decreases for both curvature parameter α and thermophoresis parameter N_t.

References

[1] S U S Choi, *ASME Int. Mech. Eng.* **66**, 99 (1995)
[2] N C Peddisetty, *Pramana – J. Phys.* **87**: 62 (2016)
[3] T Hayat, M Waqas, S A Shehzad and A Alsaedi, *Pramana – J. Phys.* **86**, 3 (2016)
[4] K M Shirvan, R Ellahi, M Mamourian and M Moghiman, *Int. J. Heat Mass Transfer* **107**, 1110 (2017)
[5] T Hayat, M Rashid, M Imtiaz and A Alsaedi, *Int. J. Heat Mass Transfer* **113**, 96 (2017)
[6] M Irfan, M Khan and W A Khan, *Results Phys.* **7**, 3315 (2017)
[7] R Ellahi, M H Tariq, M Hassan and K Vafai, *J. Mol. Liq.* **229**, 339 (2017)
[8] K K Shirvan, M Mamourian, S Mirzakhanlari and R Ellahi, *Power Tech.* **313**, 99 (2017)
[9] T Hayat, M Rashid and A Alsaedi, *Results Phys.* **7**, 3107 (2017)
[10] M Khan, M Irfan and W A Khan, *Int. J. Hydro. Energy* **42**, 22054 (2017)
[11] J A Esfahani, M Akbarzadeh, S Rashidi, M A Rosen and R Ellahi, *Int. J. Heat Mass Transfer* **109**, 1162 (2017)
[12] M Waqas, M I Khan, T Hayat and A Alsaedi, *Comput. Methods Appl. Mech. Eng.* **324**, 640 (2017)
[13] M Sheikholeslami, D D Ganji and R Moradi, *Chem. Eng. Sci.* **174**, 326 (2017)
[14] W A Khan, M Khan, M Khan, A S Alshomrani, A K Alzahrani and M S Alghamdi, *J. Mol. Liq.* **234**, 201 (2017)
[15] T Hayat, M I Khan, M Waqas and A Alsaedi, *Results Phys.* **7**, 256 (2017)
[16] S S Nourazar, M Hatami, D D Ganji and M Mhazayinejad, *Powder Tech.* **317**, 310 (2017)
[17] M Khan, M Irfan, W A Khan and L Ahmad, *Result Phys.* **7**, 1899 (2017)
[18] R Ellahi, *Appl. Sci.* **8**, (2018), https://doi.org/10.3390/app8020192
[19] A Zeeshan, N Shehzad and R Ellahi, *Results Phys.* **8**, 502 (2018)
[20] A Hamid, Hashim and M Khan, *J. Mol. Liq.* **262**, 435 (2018)
[21] L J Crane, *Z. Angew. Mat. Phys.* **26**, 619 (1975)
[22] C Y Wang, *Phys. Fluids* **31**, 466 (1988)
[23] C Y Wang and C-O Ng, *Int. J. Non-Linear Mech.* **46**, 1191 (2011)
[24] J H Markin, N Najib, N Bachok, A Ishak and I Pop, *J. Taiwan Inst. Chem. Eng.* **74**, 65 (2017)
[25] T Hayat, M I Khan, M Waqas and A Alsaedi, *J. Mol. Liq.* **231**, 126 (2017)
[26] K U Rehman, A Qaiser, M Y Malik and U Ali, *Chin. J. Phys.* **55**, 1605 (2017)
[27] M Mustafa, *Int. J. Heat Mass Transfer* **108**, 1910 (2017)
[28] M Hassan, A Zeeshan, A Majeed and R Ellahi, *J. Magn. Magn. Mater.* **443**, 36 (2017)
[29] M Khan, L Ahmad and M Ayaz, *Pramana – J. Phys.* (2018), https://doi.org/10.1007/s12043-018-1585-2
[30] T Hayat, K Rafique, T Muhammad, A Alsaedi and M Ayub, *Results Phys.* **8**, 26 (2018)
[31] M Khan, M Irfan, W A Khan and M Ayaz, *Pramana – J. Phys.* (2018), https://doi.org/10.1007/s12043-018-1579-0
[32] M Waqas, M Farooq, M I Khan, A Alsaedi, T Hayat and T Yasmeen, *Int. J. Heat Mass Transfer* **102**, 66 (2016)
[33] W A Khan, M Khan, M Irfan and A S Alshomrani, *Results Phys.* **7**, 4025 (2017)

[34] T Hayat, M Rashid, A Alsaedi and B Ahmad, *Results Phys.* **8**, 1104 (2018)
[35] T Hayat, M Waqas, M I Khan and A Alsaedi, *J. Mol. Liq.* **225**, 302 (2017)
[36] M Khan, M Irfan and W A Khan, *Results Phys.* **9**, 851 (2018)
[37] M Irfan, M Khan, W A Khan and M Ayaz, *Phys. Lett. A* **382**, 1992 (2018)
[38] A Ishak and R Nazar, *Eur. J. Sci. Res.* **36**, 22 (2009)
[39] E M A Elbashbeshy, T G Emam, M S El-Azab and K M Abdelgaber, *Int. J. Phys. Sci.* **24**, 3067 (2012)
[40] V Poply, P Singh and A V Yadav, *Alex. Eng. J.* (2017), https://doi.org/10.1016/j.aej.2017.05.025
[41] W A Khan and I Pop, *Int. J. Heat Mass Transfer* **53**, 2477 (2010)
[42] C Y Wang, *J. Appl. Math. Mech., (ZAMM)* **69**, 418 (1989)
[43] R S R Gorla and I Sidawi, *Appl. Sci. Res.* **52**, 247 (1994)